Ternary alkali stannosilicate glasses: a Mössbauer and neutron diffraction study

2000 J. Phys.: Condens. Matter 12 213

(http://iopscience.iop.org/0953-8984/12/3/302)

J. Phys.: Condens. Matter **12** (2000) 213–230. Printed in the UK PII: S0953-8984(00)07066-1

Ternary alkali stannosilicate glasses: a Mössbauer and neutron diffraction study

J A Johnson†, C E Johnson‡§, D Holland‖, A Sears‖, J F Bent‖,
P G Appleyard¶, M F Thomas‡ and A C Hannon+

† Intense Pulsed Neutron Source, Argonne National Laboratory, Argonne, IL 60439, USA
‡ Advanced Photon Source, Argonne National Laboratory, Argonne, IL 60439, USA
§ Department of Physics, University of Liverpool, Liverpool L69 3BX, UK
‖ Department of Physics, University of Warwick, Coventry CV4 7AL, UK
¶ School of the Built Environment, Liverpool John Moores University, Liverpool L3 5UG, UK
+ ISIS Facility, Rutherford Appleton Laboratory, Chilton, Didcot, Oxon OX11 0RA, UK

Received 18 August 1999

Abstract. Neutron diffraction and Mössbauer spectroscopic measurements have been performed on four series of ternary alkali stannosilicate glasses of nominal composition $(SnO_{0.5-x}(M_2O)_x(SiO_2)_{0.5}$ with $0 \leqslant x \leqslant 0.2$, where the modifier cations were M = Li, Na, K and Rb. The data show that the tin is predominantly three co-ordinate and that the length of the Sn–O bond and the O–Sn–O angle decrease with increasing modifier concentration x. This reduction increases with increasing size of the modifier cation, and is opposite in sign to the macroscopic molar volume which increases with modifier content. The ^{119}Sn Mössbauer spectra of these samples showed that most of the tin is in the Sn^{2+} state and that the isomer shift and quadrupole splitting vary approximately linearly with the Sn–O bond length and O–Sn–O bond angle for each series. This is consistent with a contraction of the 5p electron orbitals of the tin atoms and an increase in the symmetry of the ligand environment as modifier ions are added.

1. Introduction

The study of tin in float glass is technically important because the tin which diffuses into the lower surface of the glass ribbon which moves over the molten tin during manufacture can have a profound influence on the properties of the glass. Because the process takes place in a reducing atmosphere the tin enters the glass in the Sn^{2+} state and its subsequent oxidation to Sn^{4+} causes a wrinkling of the surface and hence a deterioration of the optical clarity.

The object of this work is to study the state of tin in float glass, and also to investigate the effect of modifier atoms in tin silicate glasses. Modifiers such as sodium and calcium are added to commercial glasses in order to lower the viscosity, the glass transition, and melting temperatures.

Neutron scattering is a powerful method for studying the structure (bond lengths and co-ordination numbers) of glasses. Mössbauer spectroscopy provides information on the oxidation states from the isomer shift and local structure from the quadrupole splitting. Far more detailed information is necessary to calibrate the isomer shift, especially as float glass is a multi-component system, containing Na, K, Ca and Mg as modifiers added to SiO_2.

In previous work [1] we have prepared and characterized a series of binary SnO–SiO_2 glasses containing up to 70 mol% SnO, and have studied them using Mössbauer spectroscopy [2] and neutron scattering [3]. The tin was mostly in the Sn^{2+} state and appeared to be a

0953-8984/00/030213+18$30.00

conditional glass former. For high concentrations it was predominantly co-ordinated to three oxygen neighbours, though at lower concentrations some four-co-ordination occurred.

We have extended the work to ternary SnO–SiO_2–M_2O glasses and in this paper we report the use of both neutron scattering and the ^{119}Sn Mössbauer effect to study ternary silicate glasses with composition $(SnO_{0.5-x}(M_2O)_x(SiO_2)_{0.5}$; where M_2O represents alkali modifiers (Li_2O, Na_2O, K_2O and Rb_2O) replacing the tin in the nominally equimolecular glass $(SnO)_{0.5}(SiO_2)_{0.5}$.

2. Experimental details

2.1. Specimen preparation

Four series of glasses with the general nominal formula $(SnO_{0.5-x}(M_2O)_x(SiO_2)_{0.5}$ were prepared, where M was an alkali metal (Li, Na, K and Rb).

The details of the starting materials and the preparation conditions and methods have been described in another paper [4] which also reports measurements of their densities, molar volumes, thermal expansivities, thermal stabilities and glass transition temperatures.

2.2. Neutron scattering

Neutron diffraction measurements on the Li, Na and Rb glasses were carried out using GLAD (Glass, Liquids and Amorphous materials Diffractometer) at IPNS (the Intense Pulsed Neutron Source) at Argonne National Laboratory. The crushed glasses were loaded into thin-walled vanadium tubes. Time-of-flight diffraction data were collected in groups of detectors at scattering angles ranging from 4 to 117° using momentum transfers (Q) from 0.3 up to 30 Å^{-1}. The counts were corrected for background as previously described [5] to yield the neutron weighted average structure factor $S(Q)$. Neutron measurements on the K glasses were carried out at LAD (the Liquid and Amorphous Diffractometer) at ISIS at the Rutherford Appleton Laboratory. The scattering angles ranged from 5 to 180° and Q from 0.25 to 50 Å^{-1}.

Total real space correlation functions $T(r)$ were evaluated by Fourier transformation:

$$T(r) = 4\pi\rho_0 r + \frac{2}{\pi}\int_{Q_{\min}}^{Q_{\max}} [S(Q) - 1] \sin Qr \, Q \, \mathrm{d}Q \tag{1}$$

where ρ_0 is the total number density. A Lorch modification function was used to reduce termination effects associated with the cutoff at $Q_{\max}$.

2.3. Mössbauer spectroscopy

Mössbauer spectra were collected using a conventional constant acceleration drive at Liverpool. The velocity drive was calibrated using a ^{57}Co source and an absorber of natural iron at room temperature. The γ-ray source was ^{119m}Sn in $CaSnO_3$, and the shifts are quoted relative to SnO_2 at room temperature by adding 0.11 mm s^{-1} to the observed value. The detector was a liquid nitrogen cooled intrinsic germanium solid state detector. The temperature of the glass absorbers could be varied with a continuous-flow liquid helium cryostat. The spectra were computer fitted to yield values of the shift, quadrupole splitting and f-factor.

Table 1. Analysed mole fraction compositions, molar volumes V_m and thermal expansivities β of the glasses studied.

M	x	SnO	SiO_2	V_m (10^{-6} m^3)	β (10^{-5} K^{-1})
Li	0.042	0.411	0.546	25.07	1.55
	0.086	0.374	0.540	24.03	1.90
	0.140	0.370	0.489	24.74	2.62
	0.159	0.423	0.418	24.74	2.62
	0.167	0.289	0.544	23.32	2.95
	0.208	0.230	0.546	22.89	2.75
Na	0.025	0.441	0.534	25.5	1.90
	0.049	0.450	0.500	26.25	
	0.126	0.317	0.557	24.89	3.00
	0.204	0.252	0.544	25.00	
	0.245	0.208	0.547		
	0.252	0.252	0.507	26.53	
K	0.050	0.358	0.592	26.30	1.98
	0.097	0.311	0.592	26.83	2.95
	0.185	0.223	0.593	28.61	3.79
	0.199	0.239	0.562	28.12	4.20
Rb	0.054	0.357	0.588	26.13	1.87
	0.124	0.311	0.564	29.17	3.06
	0.181	0.260	0.558	30.27	3.68

3. Results

3.1. Samples

The samples prepared were confirmed to be amorphous within the detection limits of the x-ray diffraction technique. The nature of the preparation method and the effects of oxidation and disproportionation of Sn(II) mean that there are deviations from the nominal stoichiometry, although identical conditions were found to produce consistent results. The chemical analysis was thus essential if conclusions are to be drawn about the dependence of structure upon composition. The details of the analysis have been reported earlier [4] and the analysed compositions are presented in table 1, along with the molar volumes deduced from density measurements.

3.2. Neutron scattering

3.2.1. Structure factors. Neutron structure factors $S(Q)$ obtained for the sodium stannosilicate series are presented in figure 1, showing the effect of increasing sodium content. A comparison of $S(Q)$ for all four alkali stannosilicates is made in figure 2 for glasses with an alkali content of $\sim$20%. The higher Q regions show little change on the addition of increasing amounts of alkali metal oxide; however, the features in the region of the first sharp diffraction peak (FSDP) become increasingly detailed as the concentration of alkali metal is increased. The effect is more pronounced with the larger alkali metals such as potassium and rubidium. This is in contrast with previous studies of transition metals in ternary sodium silicate glasses [5] which show large changes up to $\sim$10 Å^{-1} and a small splitting of the FSDP with increasing transition metal ion.

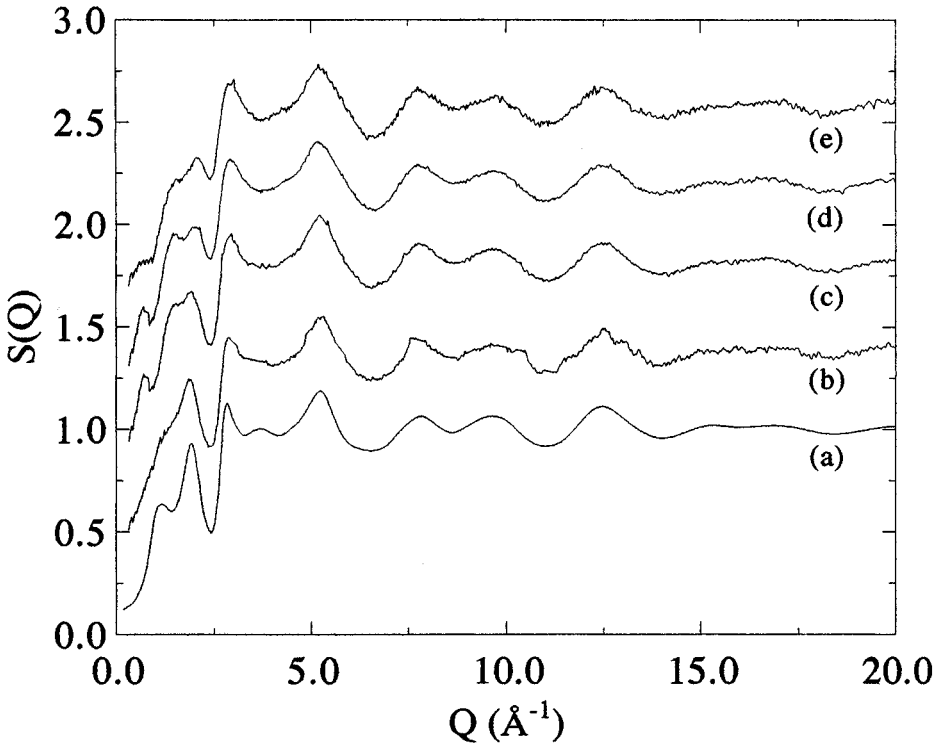

Figure 1. Structure factors $S(Q)$ for sodium stannosilicate glasses containing (a) 0%, (b) 5%, (c) 12.5%, (d) 20% and (e) 25% Na_2O. Successive curves are displaced vertically by 0.5 for clarity.

3.2.2. The first sharp diffraction peak. The FSDP occurs at a wavevector Q_1 and gives information on the intermediate range order (IRO) [6], and is substantially affected by the addition of modifier ions. For vitreous silica the addition of lithium oxide has only a small effect on the diffraction pattern [7] while potassium or rubidium oxide introduces additional structure in the region of the FSDP. For the larger atoms the addition of only a few per cent of modifier ion gives rise to the 'extended range order' peak (EROP) at a wavevector Q_0 below that of the FSDP. This has been seen before in alkali silicate glasses without tin [8]. It is, however, interesting to note that the sodium stannosilicate diffraction pattern closely resembles that of potassium silicate and potassium stannosilicate that of rubidium silicate, as if the addition of tin displaces the behaviour of the glass to that of the alkali modifier ion in the next row of the periodic table. The most interesting result, however, is in the sodium stannosilicates which show a peak in $S(Q)$ even below Q_0 termed Q_{00}.

The values of Q_1, Q_0 and Q_{00} are given in table 2 along with their corresponding characteristic repeat distances $2\pi/Q_1$, $2\pi/Q_0$ and $2\pi/Q_{00}$. The first feature in the structure factors is the peak between $Q_1 = 1.63$ Å^{-1} and 2.00 Å^{-1}, corresponding to a correlation length $L_1 = 2\pi/Q_1$ between 3.04 and 3.86 Å which is smaller than the characteristic value for oxide glasses of 4.1 Å. On the addition of the sodium, potassium and rubidium modifiers a new peak appears at Q_0 which has small changes in position and increases in intensity with increasing modifier concentration. This gives longer correlation lengths between 4.27 and 5.87 Å. The sodium structure factor seems to be unique in this series in that it shows structure at a value Q_{00} between 0.67 and 0.7 Å^{-1} giving correlation lengths between 8.98 and 9.38 Å.

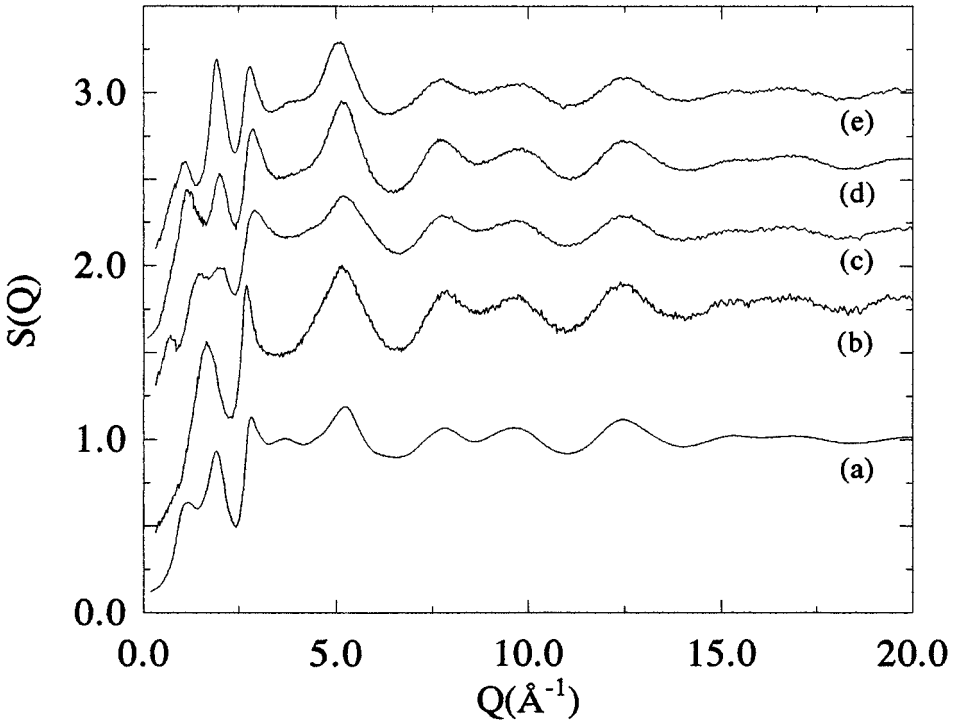

Figure 2. $S(Q)$ for alkali stannosilicate glasses containing (a) 0% alkali, (b) 20.8% Li_2O, (c) 20.4% Na_2O, (d) 19.9% K_2O and (e) 18.1% Rb_2O (nominally 20% of each alkali).

Table 2. Positions of the features at low Q of the structure factor $S(Q)$ (FSDP).

M	x	Q_{00} (Å^{-1})	$2\pi/Q_{00}$ (Å)	Q_0 (Å^{-1})	$2\pi/Q_0$ (Å)	Q_1 (Å^{-1})	$2\pi/Q_1$ (Å)
Li	0.042					1.78	3.49
	0.086					1.69	3.72
	0.140					1.65	3.81
	0.167					1.63	3.86
	0.208					1.63	3.86
Na	0.049					1.88	3.34
	0.126	0.70	8.98	1.42	4.43	1.89	3.32
	0.204	0.69	9.11	1.46	4.30	2.00	3.14
	0.252	0.67	9.38	1.47	4.27	2.07	3.04
K	0.050			1.15	5.46	1.86	3.38
	0.097			1.17	5.37	1.88	3.34
	0.199			1.18	5.33	2.00	3.14
Rb	0.054			1.07	5.87	1.88	3.34
	0.124			1.08	5.82	1.89	3.32
	0.181			1.13	5.56	1.92	3.27

3.2.3. Correlation functions. The correlation functions $T(r)$ are shown in figure 3 for the glasses with nominal alkali concentration of 20%, and representative fitted spectra are shown in figure 4. The peaks at approximately 1.6, 2.1 and 2.6 Å are identified as being due to Si–O, Sn–O and O–O correlations respectively. Na–O correlations were also observed, though the peaks are weak owing to overlap with other peaks and to low b-values. Lithium has a small

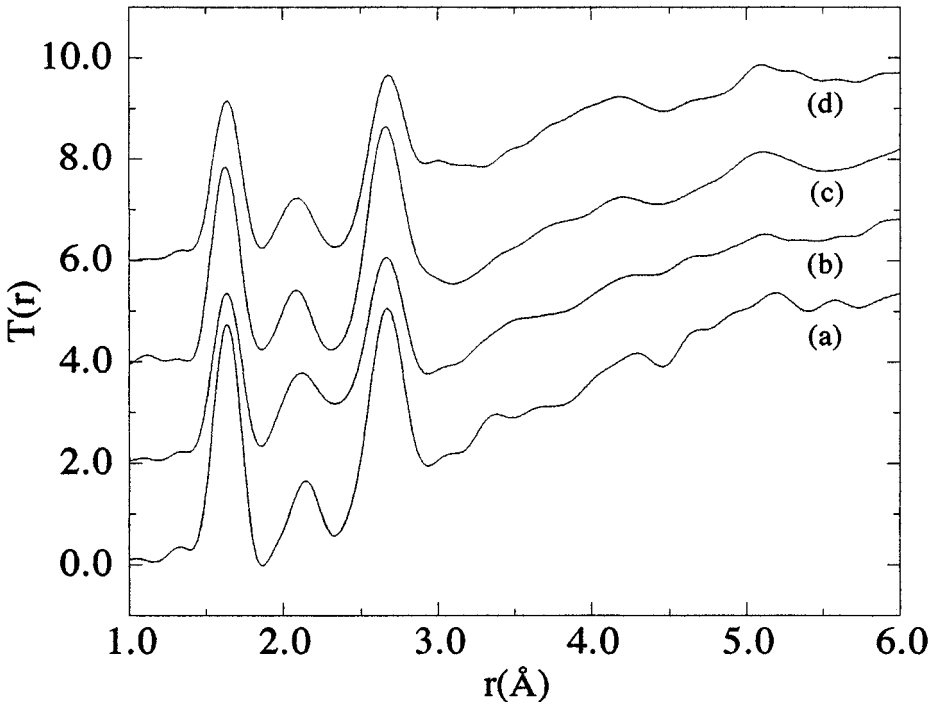

Figure 3. Correlation functions $T(r)$ for alkali stannosilicate glasses containing (a) 2.08% Li, (b) 20.4% Na_2O, (c) 19.9% K_2O and (d) 18.1% Rb_2O. Successive curves are displaced vertically by 2.0 for clarity.

and negative scattering length and so the Li–O peak is not detected in these spectra. We can, however, see that the Si–O peak reduces in area with increasing lithium concentration due to this negative peak. A typical bond length for Li–O is 1.94 Å and the co-ordination number for oxygens around lithium is 2.0 in alkali silicate glasses [9]. The K–O bond distance is 2.66 Å which is almost identical with the O–O bond distance and so cannot be distinguished from this peak. However, an approximate co-ordination number of 4.0 has been proposed for oxygens around potassium [9].

In crystalline structures the Rb–O bond distance is ∼2.9 Å. In the present data there is a peak beyond the O–O peak which increases in intensity and decreases in bond distance with increasing rubidium concentration. This peak is attributed at least partly to Rb–O correlations as Rb has a fairly large scattering length and we would expect to see something of the peak. Although the peak is not well enough resolved to give a convincing fit the co-ordination number is estimated to lie between 4 and 5.

The Na–O bond distance is ∼2.3 Å so while there is some overlap with the Sn–O peak prior experience [5] allows us to provide a fit to the sodium stannosilicates for the four peaks Si–O, Sn–O, Na–O and O–O.

The values of the bond lengths for all the alkali stannosilicates are given in table 3. The data agree well with and show the same trends as that of Hannon *et al* [9] for a lithium and a potassium silicate glass, Wright *et al* [10] for a potassium and a series of sodium silicate glasses and Johnson *et al* [5] for iron sodium silicate glasses.

The variation of the bond length R_{Sn-O} with composition is shown in figure 5, and is plotted against concentration of SnO thus enabling a comparison with the data obtained by Bent *et al* [3] on the binary SnO–SiO_2 system.

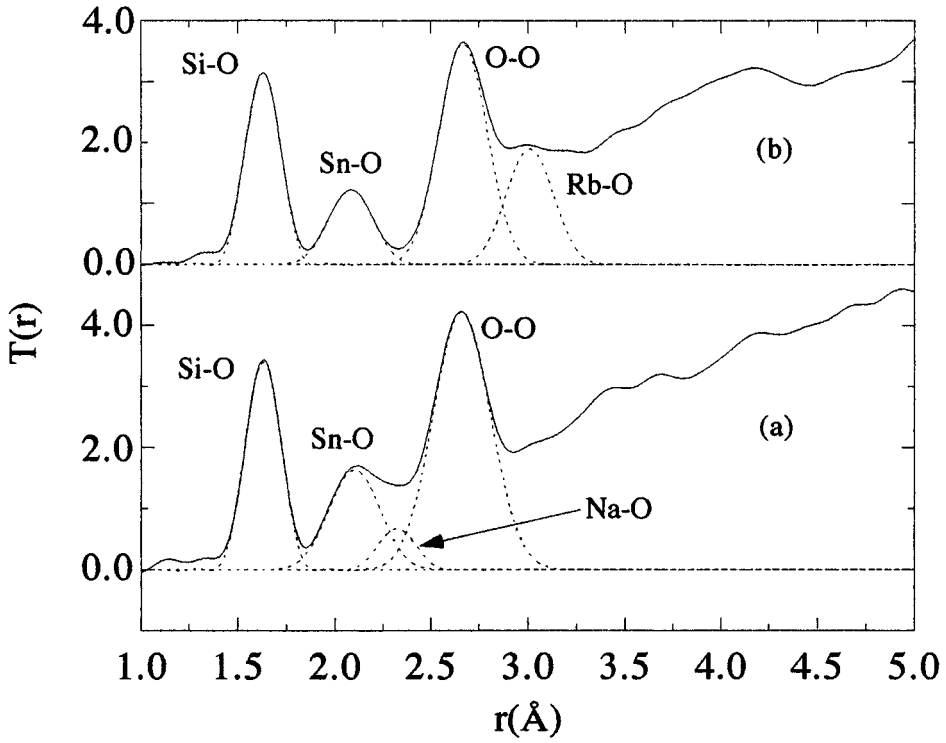

Figure 4. Correlation functions $T(r)$ for stannosilicate glasses containing (a) 5.4% Na_2O and (b) 18.1% Rb_2O with Gaussians fitted to the peaks, showing the contributions for each bond.

Table 3. Bond lengths, co-ordination numbers and bond angles deduced from neutron scattering data.

	x	R_{Si-O} (Å)	C_{Si-O}	R_{Sn-O} (Å)	C_{Sn-O}	R_{M-O} (Å)	C_{M-O}	R_{O-O} (Å)	C_{O-O}	θ_{O-Sn-O}	θ_{O-Si-O}
Li	0.042	1.622	3.8	2.135	3.2	—	—	2.658	5.3	77.0	110.0
	0.086	1.623	3.6	2.133	3.2	—	—	2.663	5.1	77.3	110.2
	0.140	1.626	3.6	2.128	2.9	—	—	2.677	5.1	78.0	110.2
	0.167	1.625	3.6	2.137	3.3	—	—	2.672	5.0	77.4	110.6
	0.208	1.627	3.5	2.134	3.0	—	—	2.672	5.1	77.5	110.4
Na	0.049	1.626	3.6	2.119	3.0	2.351	2.5	2.645	5.7	77.2	108.8
	0.126	1.625	3.5	2.097	3.8	2.341	2.6	2.661	5.2	78.8	109.9
	0.204	1.629	3.5	2.089	4.1	2.337	2.5	2.666	5.1	79.3	109.8
	0.252	1.631	3.7	2.073	3.3	2.287	2.4	2.662	5.9	79.2	109.4
K	0.050	1.622	3.9	2.119	3.1	—	—	2.657	5.2	77.7	110.0
	0.097	1.625	3.7	2.103	3.1	—	—	2.651	5.0	78.1	109.3
	0.199	1.626	3.7	2.095	2.8	—	—	2.655	5.0	78.6	109.5
Rb	0.054	1.621	3.8	2.111	3.4	—	—	2.657	5.0	78.0	110.1
	0.124	1.624	3.6	2.089	3.3	—	—	2.666	5.0	79.3	110.3
	0.181	1.629	3.8	2.083	3.4	—	—	2.676	5.4	79.9	110.4

The mean bond angles θ_{O-X-O} were deduced from the formula

$$\theta_{O-X-O} = 2\sin^{-1}\frac{R_{O-O}}{2R_{X-O}} \tag{2}$$

and θ_{O-Sn-O} is plotted against tin concentration in figure 6.

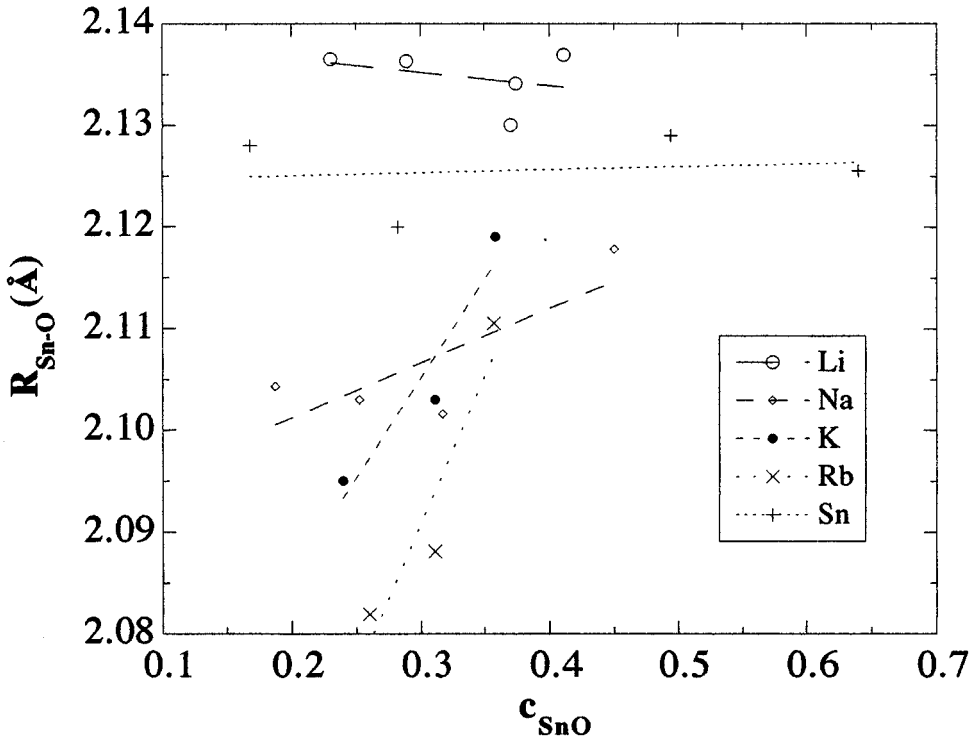

Figure 5. Variation of R_{Sn-O} with SnO concentration.

The co-ordination numbers C are deduced from the areas (A_{ij}) of the peaks, and are given by

$$C_{ij} = A_{ij}\frac{\langle\bar{b}\rangle^2}{b_i b_j}\frac{1}{2c_i} \qquad \text{and} \qquad C_{ii} = A_{ii}\frac{\langle\bar{b}\rangle^2}{b_i^2 c_i} \tag{3}$$

where the b are the scattering lengths and c_i the concentration of element i. The values for C_{Si-O}, C_{Sn-O}, C_{O-O} and C_{Na-O} are listed in table 3.

Due to the overlapping of peaks it is often difficult to determine the co-ordination number with any accuracy. However, the bond distance which can be determined to within ± 0.01 Å, and in many cases better, can be used with estimates from bond valence calculations to determine co-ordination number. Bond valence parameters relate bond valencies and bond lengths through the equation

$$R_{i-j} = r_{ij} - a\ln\frac{V_i}{c_{ij}} \tag{4}$$

where a is a universal constant $= 0.37$ Å, V_i is the valency and r_{ij} is the bond distance parameter and is taken from the tables of Brese and O'Keefe [11]. Using (4) for $V_i = 2$ and $r_{ij} = 1.984$ Å, three co-ordination gives $R_{Sn-O} = 2.134$ Å in close agreement with what is found, whereas four co-ordination would give $R_{Sn-O} = 2.240$ Å which is much greater than any tin–oxygen bond length observed in stannosilicate glasses..

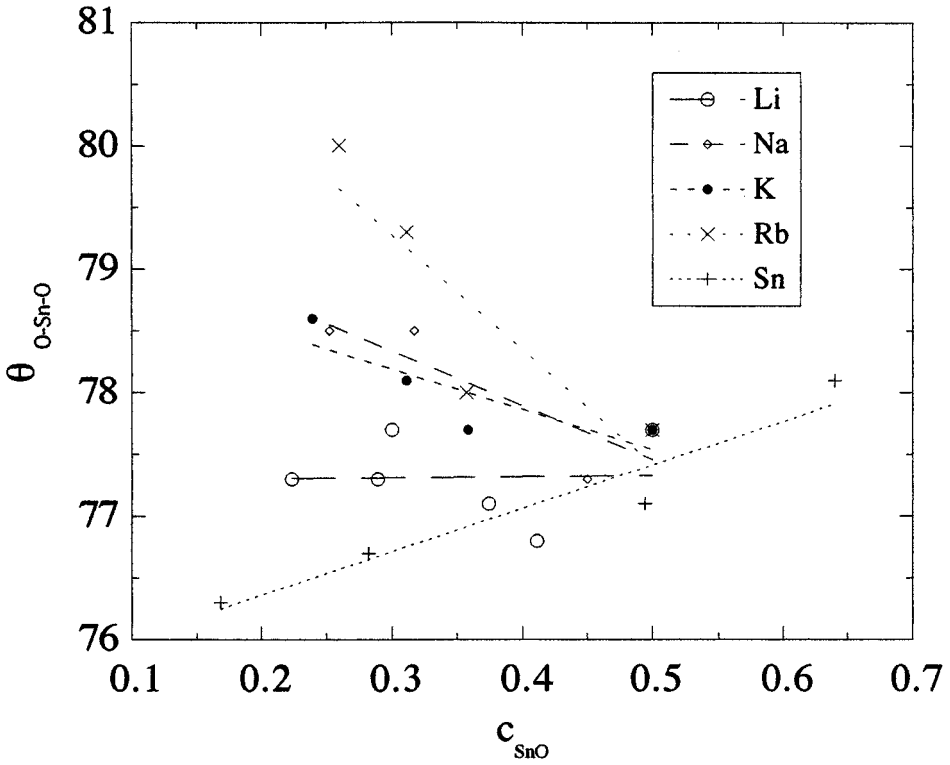

Figure 6. Variation of θ_{O-Sn-O} with SnO concentration.

3.3. Mössbauer spectra

Figure 7 shows the Mössbauer spectra at 77 K of the sodium stannosilicate glasses for different sodium concentrations. The other alkali modifiers give similar spectra, and show that most of the tin is in the Sn^{2+} state. As the modifier concentration is increased (or the tin concentration is decreased) there is an increasing but still small fraction of Sn^{4+} present.

The shifts δ of the Sn^{2+} relative to SnO_2 and quadrupole splittings Δ deduced from the spectra are plotted in figures 8 and 9 respectively as a function of the SnO concentration for each series.

Table 4. Values of $\partial\delta/\partial T$, $\partial\delta^I/\partial T$, $\partial\delta/\partial T$ and θ_D for different glasses from variable temperature Mössbauer spectra.

M	x	$\partial\delta/\partial T$ (10^{-4} mm s^{-1} K^{-1})	$\partial\delta^I/\partial T$ (10^{-4} mm s^{-1} K^{-1})	$\partial\Delta/\partial T$ (10^{-4} mm s^{-1} K^{-1})	Θ_D (K)
Li	0.159	−2.96	0.541	−2.397	210.2
	0.208	−2.63	0.861	−2.117	205.2
Na	0.025	−2.35	1.148	−1.880	172.4
	0.245	−3.21	0.283	−2.410	186.2
K	0.050	−3.08	0.419	−2.310	182.6
	0.185	−3.30	0.196	−2.266	183.6
Rb	0.054	−3.06	0.440	−3.316	185.9
	0.181	−2.69	0.803	−2.850	173.2

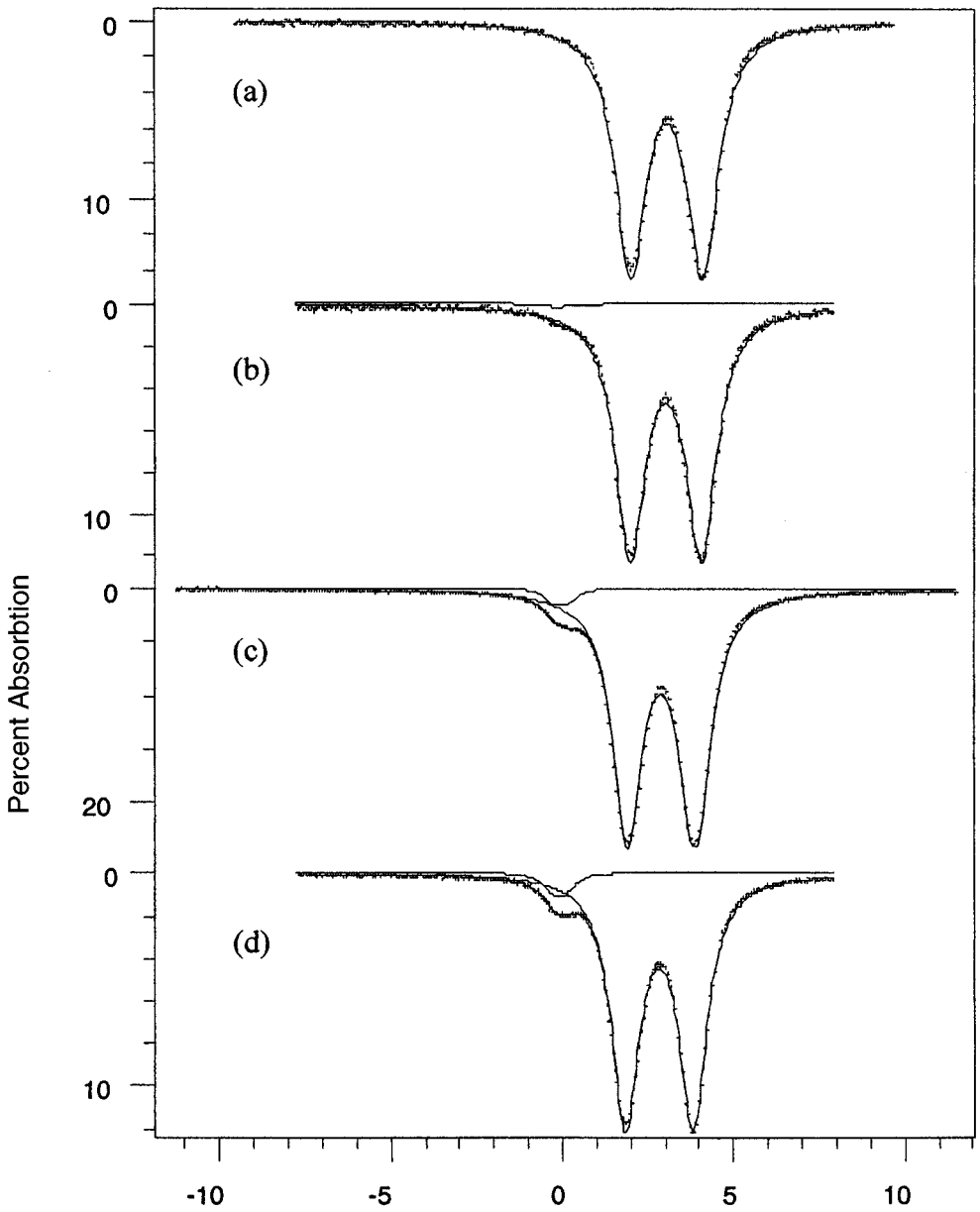

Figure 7. Mössbauer spectra of sodium stannosilicate glasses at 77 K. The zero of the velocity scale is relative to SnO_2.

The spectra were also measured as a function of temperature. The shift δ comprises two contributions

$$\delta = \delta^{SOD} + \delta^{I} \tag{5}$$

where δ^{SOD} is the second order Doppler shift resulting from atomic motion and becomes more negative as the temperature is increased, and δ^{I} is the isomer shift proportional to the electron density at the nucleus. Since the variation of δ^{SOD} with temperature may be

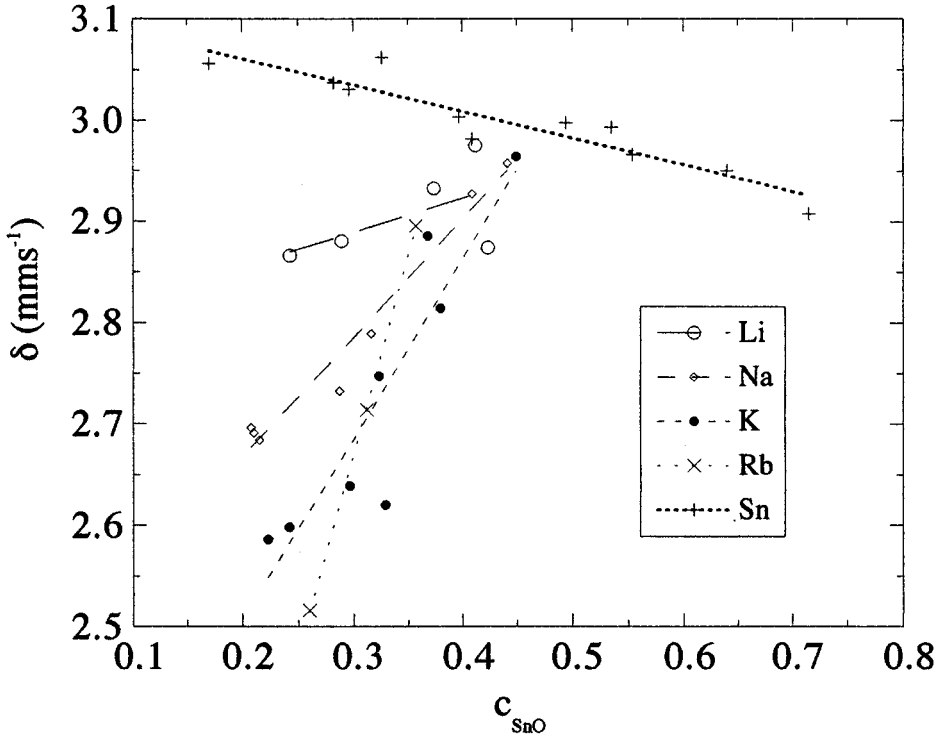

Figure 8. Sn^{2+} Mössbauer shifts at 77 K as a function of SnO concentration for alkali stannosilicate glasses.

calculated, δ^I may be deduced from the data: at temperatures above the Debye temperature $\partial\delta^{SOD}/\partial T = -3.5 \times 10^{-4}$ mm s^{-1} K^{-1}. The observed $\partial\delta/\partial T$ is less steep than this for all the glasses and hence $\partial\delta^I/\partial T$ is positive. The increase in δ^I with increasing temperature, i.e. decreasing density, shows that the s electrons are shielded by the 5p electrons. Values for the slopes $\partial\delta/\partial T$ and $\partial\delta^I/\partial T$ found for the glasses studied are given in table 4. The consistency between the values of these slopes is not always reliable owing to the variable amounts of tin and silicon present, but they are good enough for an estimate of the correction to be applied to the isomer shift due to changes in volume.

4. Discussion

4.1. Neutron structure factors

The potassium and rubidium glasses behave in a very similar manner and have close values of Q_0 and Q_1 and hence repeat distances. The rubidium repeat distances are slightly longer, probably due to the larger atoms. In rubidium germanate glasses the modifier is thought to go into the cages and displace oxygen atoms on their boundaries [12] leading to a strong diffraction peak at Q_0. The cages without the Rb^+ will correspondingly contract and so account for the increase in Q_1. It is surmised that a similar effect occurs in the potassium and rubidium stannosilicate glasses. The lithium stannosilicates show little structural change: Q_1 in fact moves to a lower value as more modifier is added. Clearly there is a different structural role for lithium which can be explained with reference to the correlation functions in section 4.2.

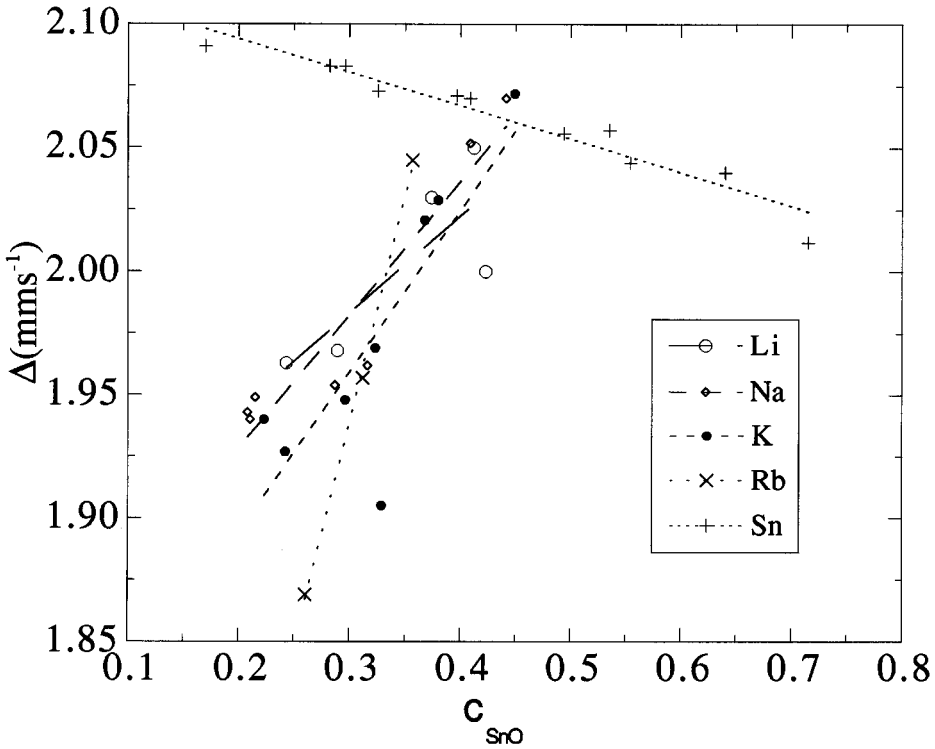

Figure 9. Sn^{2+} quadrupole splittings at 77 K as a function of SnO concentration for alkali stannosilicate glasses.

The behaviour of Q_1 in the sodium glasses is similar to that of the potassium and rubidium glasses but there are two peaks at very low Q, Q_0 and Q_{00}, where the value of Q_0 increases as more modifier is added and Q_{00} has the opposite trend. It is likely that sodium has a mixture of roles to play which lies between that of lithium and the larger atoms.

The overall behaviour of these glasses is thus close to that of alkali silicate glasses in the absence of tin. This is not surprising as previous work [3] has established that tin is a conditional network former and substitutes for silicon in the network.

4.2. Correlation functions and bond lengths

The structure factor data have already indicated that potassium and rubidium go into the cages of the glass network, and that this is also partially the role of sodium. Lithium is thought, however, to sit in pairs between two non-bridging oxygens (NBOs) in alkali silicate glasses from co-ordination number data [9]. In this paper we suggest that this is also the case for lithium and partly for sodium in stannosilicate glasses.

The Si–O and O–O bond lengths are seen from table 3 to decrease slightly as the tin concentration is increased. The O–Si–O angle remains close to the ideal tetrahedral value. A similar variation was observed in the binary stannosilicate glasses [3]. It is difficult to obtain accurate data as the oxygen peak in the correlation function does not allow resolution of the Si and Sn polyhedra, so the average value of the O–O bond lengths has been assumed to apply to both.

Table 5. Measured values of $\partial R_{Sn-O}/\partial c_M$ for different alkali modifiers, and radii r_M of modifier ions. Values of r_M are taken from Shannon R D and Prewitt C T 1970 *Acta Crystallogr.* B **26** 1046.

	$\partial R_{Sn-O}/\partial c_M$ (10^{-2} Å mol^{-1})	$\partial R_{Sn-O}/\partial c_{SnO}$ (10^{-2} Å mol^{-1})	$\partial V_m/\partial c_{M_2O}$ (10^{-2} Å mol^{-1})	$\partial V_m/\partial c_{SnO}$ (10^{-2} Å mol^{-1})	r_M (Å)
Li_2O	−0.006	−0.013	−0.121	0.0971	0.74
Na_2O	−0.085	0.053	−0.013	0.0119	1.02
K_2O	−0.140	0.194	0.1474	−0.112	1.38
Rb_2O	−0.229	0.291	0.2866	−0.198	1.49

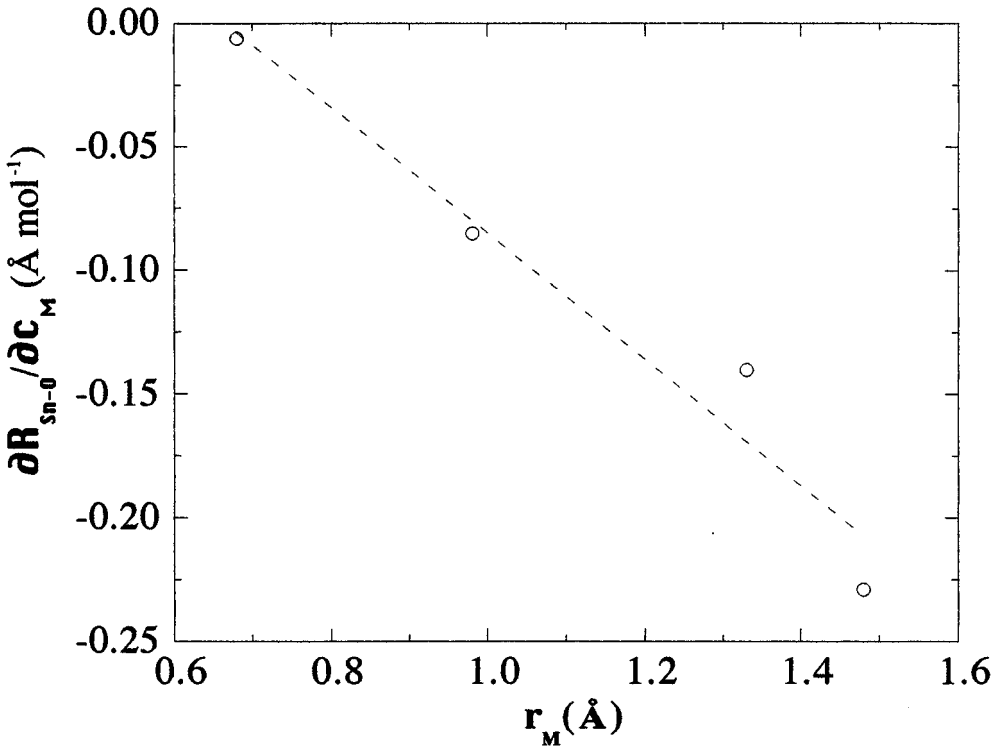

Figure 10. Rate of change of R_{Sn-O} with SnO concentration as a function of r_M, the radius of the modifier ion.

As modifier atoms are substituted for tin the bond lengths R_{Sn-O} decrease, except for Li which produces a slight increase. Since the Sn–O bond length is almost constant in binary stannosilicate glasses [3] the change must be primarily due to the effect of the modifier cation. The slopes $\partial R_{Sn-O}/\partial c_M$ are given in table 5 and are plotted against r_M, the ionic radius of the modifier, in figure 10 yielding a straight line. Hence the larger the modifier ion is the more compact does the polyhedron around the tin become. The modifier squashes the oxygens around the tin.

It is interesting to note that the changes in the local dimensions in the region of the tin atoms are inversely related to the changes in molar volume calculated from the bulk densities and given in table 1. An expansion of the network coincides with a contraction of the Sn–O bond length. The O–Sn–O angle (figure 6) also decreases with increasing tin concentration.

4.3. Mössbauer isomer shift

The Mössbauer isomer shift is a measure of the s-electron density at the nucleus, and depends upon the oxidation state and degree of covalency of the atom. For ^{119}Sn the shift is found to decrease when pressure is applied [13], i.e. when the density increases, which shows the shielding effect of the p electrons. This is also clear from the temperature dependent data (section 3.3). Thus an increase in δ implies an increase in molar volume and/or the co-ordination number.

As modifier atoms are substituted for tin, δ decreases linearly, the reduction increasing in the order Li, Na, K, Rb (see figure 8). Since the Debye temperatures of all the glasses do not vary greatly the contribution to δ^{SOD} is about the same for all of them and changes in δ are the changes in δ^I. Values of $\partial\delta^I/\partial c_{SnO}$ are given in table 6, and are positive (except for Li which is small and negative). Thus the molar volume is reduced, or the electron density in the region of the tin nuclei increases proportionally to the size of the modifier ions.

The isomer shift δ^I increases with temperature, unlike δ^{SOD} which decreases. This is in accord with the increase in volume due to thermal expansion. The slope $\partial\delta^I/\partial T$ may be used to determine the contribution to $\partial\delta/\partial c_{SnO}$ due to the change in volume, since

$$\left(\frac{\partial\delta^I}{\partial c_{SnO}}\right)_T = \frac{\kappa}{\beta}\left(\frac{\partial\delta^I}{\partial T}\right)_c \tag{6}$$

where

$$\kappa = \partial \ln V/\partial c_{SnO} \tag{7}$$

is the compressibility under changes in composition and β is the thermal expansivity.

If the bulk molar volume V_m is used in (7), the correction given by (6) is negative. As noted in 4.2 the local compressibility has the opposite sign from the bulk value, and so a more appropriate volume to use in κ is the local one proportional to $(R_{Sn-O})^3$. This correction is given in table 6 together with the corrected value $\partial\delta^I/\partial c^{VC}_{SnO}$. It is seen that the correction is not large compared with the measured value but is of the right sign, so that $\partial\delta^I/\partial c_{SnO}$ remains positive in sign and $\partial\delta^I/\partial c_M$ is negative. It seems likely that the changes in δ^I are due to changes in volume and the appropriate volume to use in (7) is that of the Sn atom itself, i.e. $\langle r^{-3}\rangle_{5p}$, but we have no independent measurement of this.

4.4. Quadrupole splitting

The quadrupole splitting measures the electric field gradient at the nucleus, and increases as the molar volume decreases or as the arrangement of the ligands becomes more asymmetric.

For Sn^{2+} the dominant contribution to the electric field gradient comes from the 5p electrons, and the quadrupole splitting is given by

$$\Delta = \tfrac{2}{5}e^2Q\langle r^{-3}\rangle_{5p}\langle 3\cos^2\theta - 1\rangle_{5p}. \tag{8}$$

When the temperature is increased $\langle r^{-3}\rangle_{5p}$ decreases due to thermal expansion and hence Δ decreases as observed.

As modifier atoms are substituted for tin, Δ becomes smaller (see figure 9). The reduction of the isomer shift observed implies a reduction in local volume $\langle r^{-3}\rangle_{5p}$ for which an increase in Δ would be expected. Hence the observed reduction in Δ must be due to a decrease in the asymmetry of the ligands $\langle 3\cos^2\theta - 1\rangle_{5p}$. This in turn implies that the O–Sn–O angle must increase, which is in accord with the neutron diffraction measurement (section 4.1). The correlation between the quadrupole splitting and the O–Sn–O bond angle is illustrated in figure 11.

Table 6. Values of the slopes of δ, δ_I and Δ with respect to the concentrations of SnO and modifier.

	$\partial\delta/\partial c_{SnO}$ (10^{-2} mm s^{-1} mol^{-1})	$(\partial\delta^I/\partial c_{SnO})_T$ (10^{-2} mm s^{-1} mol^{-1})	$\partial\delta^I/\partial c^{VC}_{SnO}$ (10^{-2} mm s^{-1} mol^{-1})	$\partial\Delta/\partial c_{SnO}$ (10^{-2} mm s^{-1} mol^{-1})	$\partial\delta^I/\partial c_M$ (10^{-2} mm s^{-1} mol^{-1})	$\partial\delta^I/\partial c^{VC}_M$ (10^{-2} mm s^{-1} mol^{-1})	$\partial\Delta/\partial c_M$ (10^{-2} mm s^{-1} mol^{-1})
Li_2O	0.616	−0.069	0.685	0.324	−0.708	−0.718	−0.505
Na_2O	1.018	0.314	0.704	0.458	−1.182	−0.869	−0.520
K_2O	1.610	0.361	1.249	0.612	−2.099	−1.770	−0.814
Rb_2O	3.175	0.949	2.226	1.104	−2.443	−1.853	−0.867

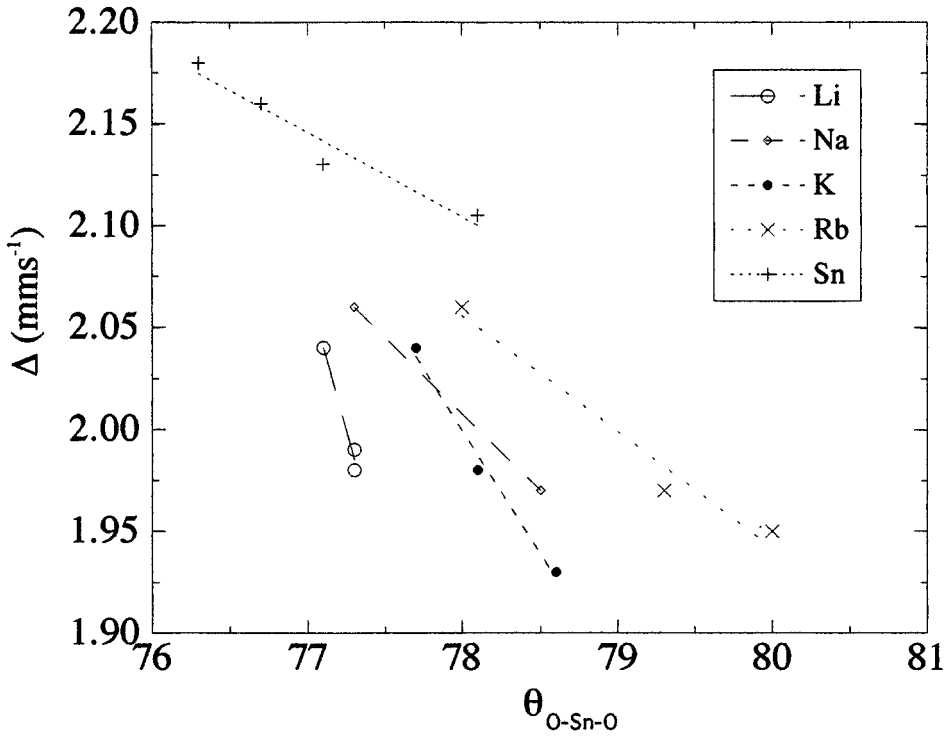

Figure 11. ^{119}Sn quadrupole splitting plotted against bond angle θ_{O-Sn-O}.

4.5. f-factor

The recoil-free fractions (f-factors) deduced from the decrease in the intensity of the spectra as the temperature was increased were measured for each glass. The change in f-factor with temperature was used to determine the effective Debye temperatures Θ_D of Sn^{2+} in the glasses, and the values are included in table 4. It is seen that Θ_D decreases as the size of the modifier cation increases.

Θ_D was also measured for the minority Sn^{4+} ions present and was found to be ~220 K for glasses containing Na_2O, i.e. larger than that of Sn^{2+}.

5. A model for the tin co-ordination

A simple model has been put forward to describe the local structure in binary [3] and ternary [4] stannosilicate glasses. It is, therefore, important to see to what extent this model can explain the observations in the present work. The tin co-ordination by three oxygens in the binary $SnO–SiO_2$ series implies that a number of oxygens, equal to the number of tin atoms, must be three-co-ordinated also ($_3O^{\delta+}$) as otherwise there is insufficient oxygen available. This gives a local unit of the type shown on the left of figure 12 where there is charge separation and the extra co-ordination is shown in the form of a dative bond.

When alkali is substituted for SnO, oxygen supplied by the modifier can be used to maintain a Sn co-ordination of three, while M^+ charge compensates the nominal $1-$ on the $[:SnO_3]$. The other product could be either bridging oxygens (figure 12(a)) or non-bridging oxygens (NBOs) (figure 12(b)). Beyond $x = 0.25$, NBOs must be formed or an increase in the tin

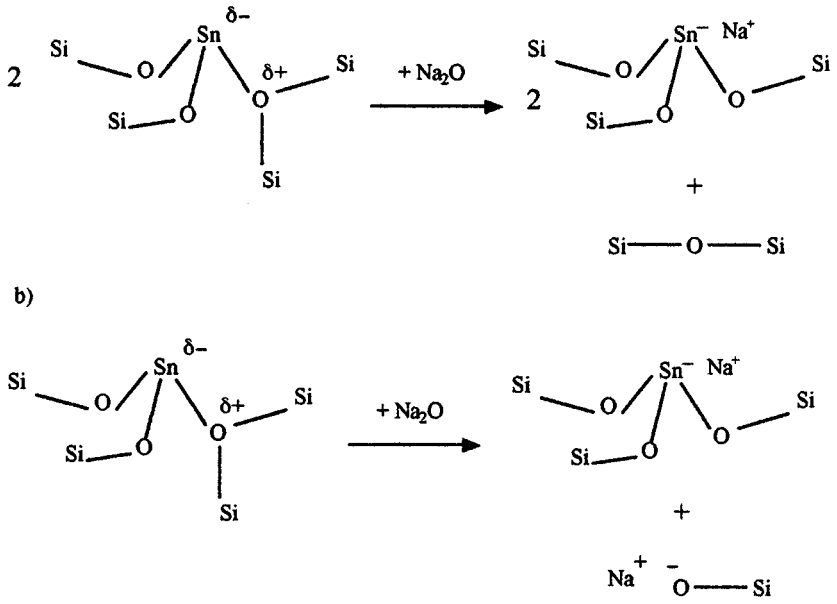

Figure 12. Models for the structure of stannosilicate glasses in the neighbourhood of the tin atoms for (a) bridging oxygens and (b) non-bridging oxygens.

co-ordination number must occur. The consequence of effective replacement of $_3O^{\delta+}$ by M^+ is that the electron density available to the bonding in the [: SnO_3] unit is increased, which results in a shortening of the Sn–O bonds. The Sn–$_3$O bond might be expected to be longer than the other two bonds and the various O–Sn–O angles non-equivalent. Thus the replacement of the $_3$O will lead to increased symmetry of the bonding about the Sn nucleus and a decrease in the quadrupole splitting Δ as observed. The variation with cation type reflects their differing polarizing power. Hence Rb^+ allows a higher effective electron density on the [: SnO_3] unit than does Li^+.

Replacement of the $_3$O by $_2$O effectively changes the local cross-linking of the network—a factor which may contribute to the change in the extended range order. It is not apparent from this model why the nature of M^+ should also affect the extended range order but steric effects will also play a part.

6. Conclusions

Neutron diffraction shows that the co-ordination number of tin in ternary stannosilicate glasses is three. The effect of the modifier alkali ions is to contract the [: SnO_3] polyhedra, even though the overall effect is to expand the bulk structure, and to decrease the O–Sn–O angle. The decrease in the Mössbauer isomer shift is mainly associated with the resulting contraction of the 5p electron orbitals of the tin atom, and the decrease in quadrupole splitting results from the increasingly symmetrical ligand environment as the O–Sn–O angle increases.

Acknowledgments

We are grateful to David Long Price for valuable discussions and critical comment. C E Johnson wishes to thank the Leverhulme Trust for the award of an Emeritus Fellowship.

This work was supported by the Division of Material Sciences, Office of Basic Energy Sciences, US Department of Energy, under contract No W-31-109-ENG-38.We also thank the Engineering and Physical Sciences Research Council for access to the ISIS Facility and for provision of a studentship to J F Bent.

References

[1] Karim M M and Holland D 1995 *Phys. Chem. Glasses* **36** 206
[2] Williams K F E, Johnson C E, Johnson J A, Holland D and Karim M M 1995 *J. Phys.: Condens. Matter* **7** 9485–97
[3] Bent J F, Hannon A C, Holland D and Karim M M 1998 *J. Non-Cryst. Solids* **232–234** 300–8
[4] Sears A, Holland D and Dowsett M G *Phys. Chem. Glasses* at press
[5] Johnson J A, Johnson C E, Holland D, Mekki A, Appleyard P and Thomas M F 1999 *J. Non-Cryst. Solids* **246** 104–14
[6] Price D L, Moss S C, Reijers R, Saboungi M L and Susman S 1989 *J. Phys.: Condens. Matter* **1** 1005
[7] Misawa M, Price D L and Suzuki K 1980 *J. Non-Cryst. Solids* **37** 85–97
[8] Price D L, private communication
[9] Hannon A C, Vessal B and Parker J M 1992 *J. Non-Cryst. Solids* **150** 97–102
[10] Wright A C, Clare A C, Bachera B, Hannon A C and Vessal B 1991 *Trans. Am. Cryst. Assoc.* **27** 239–54 (1991)
[11] Brese N E and O'Keefe M 1991 *Acta Crystallogr.* B **47** 192–7
[12] Price D L, Ellison A J G, Saboungi M L, Hu R Z, Egami T and Howells W S 1997 *Phys. Rev.* B **55** 11 249–55
[13] Panyushkin V N 1968 *Soviet Phys.–Solid State* **10** 1515